

# Motion Control for Autonomous Underwater Vehicles: A Robust Model - Free Approach

George C. Karras<sup>1</sup>, Charalampos P. Bechlioulis<sup>1</sup>, Sharad Nagappa<sup>2</sup>, Narcís Palomeras<sup>2</sup>,  
 Kostas J. Kyriakopoulos<sup>1</sup>, Marc Carreras<sup>2</sup>

**Abstract**—This paper describes the design and implementation of a robust position tracking control scheme for an Autonomous Underwater Vehicle (AUV). The proposed controller does not require knowledge of the vehicle's dynamic parameters and guarantees prescribed transient and steady state performance despite the presence of external disturbances acting on the vehicle. The resulting scheme is of low complexity and computational cost and thus can be easily integrated to an embedded control platform of an AUV. The proposed control scheme has analytically guaranteed stability and convergence properties, while its applicability and performance are experimentally verified using the Girona500 AUV into two different missions: a) navigation and stabilization to a specific configuration, b) meandrus-like trajectory tracking. In both cases the vehicle was under the influence of time-varying external disturbances caused by a high-pressure water jet installed on the Girona500 manipulator.

## I. INTRODUCTION

During the last few decades underwater vehicles are being extensively used for complex operations and dexterous tasks such as surveillance and mapping of underwater structures, ship hull inspection, handling of underwater equipment (e.g control panels, valves), search and rescue missions, etc. In most of these cases, the vehicles operate under the influence of strong external disturbances caused from ocean currents and waves. Moreover, the vehicle's dynamic parameters are likely to change, because different types of sensors and tools are utilized, depending on the requirements of each mission, for the AUV state estimation as well as the perception of the environment. Thus, the motion control scheme of an AUV should be robust against external disturbances and up to a certain extent, independent from the vehicle's dynamics.

The motion control problem for autonomous underwater vehicles has been an active research field for the past two decades and continues to pose considerable challenges to control designers especially when the vehicles exhibit large model uncertainty and are affected by environmental disturbances. A typical motion control problem is trajectory tracking which is concerned with the design of control laws that force a vehicle to reach and follow a reference trajectory.

This work was supported by the EU funded project PANDORA: Persistent Autonomy through learnIng, aDaptation, Observation and ReplAnning", FP7-288273, 2012-2014.

<sup>1</sup>School of Mechanical Engineering, National Technical University of Athens, Athens 15780, Greece {karrasg, chmpechl, kkyria}@mail.ntua.gr.

<sup>2</sup>University of Girona, Edifici Politecnica IV, Campus Montilivi, Girona 17071, Spain {snagappa, npalomer, marcc}@eia.udg.edu.

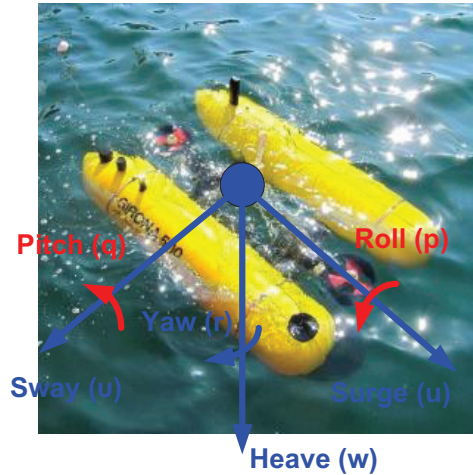


Fig. 1. The Girona500 AUV. Blue color indicates actuated DoFs. Red color indicates under actuated DoFs.

Classical approaches such as local linearization and input-output decoupling have been used in the past to design tracking controllers for underactuated vehicles [1]. Nevertheless, the aforementioned methods yielded poor closed loop performance and the results were local, around only certain selected operating points. Alternative approaches involved output feedback linearization combined with PID control, linear quadratic optimal control and  $H_\infty$  control [2]–[4], which, however, was not always possible. Finally, based on a combined approach involving Lyapunov theory and the backstepping technique various nonlinear model-based trajectory tracking controllers have been reported during the last two decades [5]–[11]. However, these schemes demand a very accurate knowledge of the vehicle dynamic parameters which in most cases is quite difficult to obtain.

Despite the recent progress in the tracking control for underwater vehicles, certain issues still remain open. Notice that even in case the actual vehicle model is considered accurately known, external disturbances affect severely the tracking performance thus making the problem of guaranteeing prescribed performance difficult or impossible in certain situations. The term prescribed performance actually means that the tracking error should converge to a predefined arbitrarily small residual set with convergence rate no less than a prespecified value. The tracking performance deterioration becomes more intense when uncertainty in the vehicle model is also present.

In this paper, a novel position and trajectory tracking

control scheme for an Autonomous Underwater Vehicle is presented. The proposed controller does not utilize the vehicle's dynamic model parameters and guarantees prescribed transient and steady state performance despite the presence of external disturbances. Moreover, through the appropriate selection of certain performance functions, the proposed scheme can also guarantee the satisfaction of motion and performance constraints imposed by the desired task. In this work, the applicability and performance of the proposed scheme are depicted using the Girona500 AUV (Fig. 1) operating in two different tasks: a) navigation and stabilization to a specific configuration, b) meandrus-like trajectory tracking. In order to prove the robustness of the system, a water jet equipment was installed on the Girona500 manipulator. During the experiments, the manipulator was moving in different directions with the water jet running, imposing strong time-variant and multidirectional external disturbances on the vehicle.

## II. PRELIMINARIES

### A. AUV Kinematics and Dynamics

In this work, we consider the Girona500 autonomous underwater vehicle (see Fig. 1). A simplified 3D dynamic model (in surge, sway, heave and yaw) of the vehicle is presented in this subsection in accordance to the standard underwater vehicle modeling properties [12]. The roll and pitch degrees of freedom are neglected for the clarity of the presentation and owing to page limitations. It will be mentioned in the sequel, however, that the stability of both degrees of freedom can be secured owing to their Input to State Stability (ISS) properties, without compromising the achieved results. In this respect, consider the vehicle modeled as a rigid body subject to external forces and torques. Let  $\{I\}$  be an inertial coordinate frame and  $\{B\}$  a body-fixed coordinate frame, whose origin  $O_B$  is located at the center of mass of the vehicle. Furthermore, let  $(x, y, z)$  be the position of  $O_B$  in  $\{I\}$  and  $\psi$  denote the yaw angle. Let  $(u, v, w)$  be the longitudinal (surge), transverse (sway) and vertical (heave) velocities of  $O_B$  with respect to  $\{I\}$  expressed in  $\{B\}$  and  $r$  be the vehicle's angular speed (yaw) around the vertical axis. Thus, the kinematic equations of motion for the considered vehicle can be written as:

$$\dot{x} = u \cos \psi - v \sin \psi + \delta_x(t) \quad (1)$$

$$\dot{y} = u \sin \psi + v \cos \psi + \delta_y(t) \quad (2)$$

$$\dot{z} = w + \delta_z(t) \quad (3)$$

$$\dot{\psi} = r + \delta_\psi(t) \quad (4)$$

where  $\delta_x(t)$ ,  $\delta_y(t)$ ,  $\delta_z(t)$ ,  $\delta_\psi(t)$  denote bounded ocean currents. Neglecting the motion in roll and pitch, the simplified equations for the surge, sway, heave and yaw can be written as:

$$m_u \dot{u} = m_v v r + X_u u + X_{|u|u} |u| u + X + \delta_u(t) \quad (5)$$

$$m_v \dot{v} = -m_u u r + Y_v v + Y_{|v|v} |v| v + Y + \delta_v(t) \quad (6)$$

$$m_w \dot{w} = Z_w w + Z_{|w|w} |w| w + (W - B) + Z + \delta_w(t) \quad (7)$$

$$m_r \dot{r} = (m_u - m_v) u v + N_r r + N_{|r|r} |r| r + N + \delta_r(t) \quad (8)$$

where  $m_u$ ,  $m_v$ ,  $m_w$ ,  $m_r$  denote the vehicle's mass, moment of inertia, added mass and moment of inertia terms,  $X_u$ ,  $X_{|u|u}$ ,  $Y_v$ ,  $Y_{|v|v}$ ,  $Z_w$ ,  $Z_{|w|w}$ ,  $N_r$ ,  $N_{|r|r}$  are negative hydrodynamic damping coefficients of first and second order,  $W$  and  $B$  are the vehicle weight and buoyancy respectively,  $\delta_u(t)$ ,  $\delta_v(t)$ ,  $\delta_w(t)$ ,  $\delta_r(t)$  denote bounded exogenous forces and torques acting on surge, sway, heave and around yaw owing to ocean waves and  $X$ ,  $Y$ ,  $Z$ ,  $N$  denote the control input forces and torque respectively that are applied by the thrusters in order to produce the desired motion of the body fixed frame.

### B. Navigation Module

The navigation module is responsible for estimating the state feedback for the control scheme and more specific the vehicle position and velocity vector. The linear positions  $([x \ y \ z])$  and velocities  $([u \ v \ w])$  are estimated using a Vision EKF SLAM algorithm, while the angular positions  $([\phi \ \theta \ \psi])$  and velocities  $([p \ q \ r])$  are directly measured using an inertial measurement unit (IMU). The Vision EKF SLAM algorithm provides simultaneously estimation updates for the visual landmarks and the linear positions and velocities of the vehicle.

The augmented system model (vehicle and landmarks) consists of a constant velocity kinematic model for the vehicle and a constant time model for the landmarks. Regarding the measurement models, position and velocity sensors are available. A global positioning system (GPS) measures the vehicle position in  $(x, y)$  plane when the vehicle is not submerged and a pressure sensor transforms pressure values into depth measurements  $(z)$ . The velocity updates are provided by a doppler velocity log (DVL). This sensor is able to measure linear velocities with respect to the sea bottom or the water around the vehicle. The pose and velocity updates are direct measurements of the state vector.

If only these two updates are available, the navigation module is a dead reckoning algorithm that drifts over time. However, if landmarks are detected in the environment, the navigation module is able to keep its position covariance bounded. A visual detection algorithm, gives information about the relative position of a landmark with respect to the vehicle. This information not only updates the detected landmarks position but also the vehicle's. The visual detection algorithm uses an *a priori* known template to identify and compute the relative position of these landmarks. During the experiments an underwater panel was used as the main landmark. The mathematical description of the navigation module and the Vision EKF SLAM algorithm are out of the scope of this paper and thus are omitted.

### C. Prescribed Performance

It will be clearly demonstrated in Subsection III-A, that the control design is connected to the prescribed performance notion that was originally employed to design neuro-adaptive controllers for various classes of nonlinear systems [13]–[15], capable of guaranteeing output tracking with prescribed performance. In this work, by prescribed performance, it is meant that the tracking error converges to a predefined

arbitrarily small residual set with convergence rate no less than a certain predefined value. For completeness and compactness of presentation, this subsection summarizes preliminary knowledge on prescribed performance. Thus, consider a generic scalar error  $e(t)$ . Prescribed performance is achieved if  $e(t)$  evolves strictly within a predefined region that is bounded by decaying functions of time. The mathematical expression of prescribed performance is given,  $\forall t \geq 0$ , by the following inequalities:

$$-\rho(t) < e(t) < \rho(t) \quad (9)$$

where  $\rho(t)$  is a smooth, bounded, strictly positive and decreasing function of time satisfying  $\lim_{t \rightarrow \infty} \rho(t) > 0$ , called performance function [13]. Hence, for an exponentially decreasing performance function  $\rho(t) = (\rho_0 - \rho_\infty)e^{-lt} + \rho_\infty$  with  $\rho_0, \rho_\infty, l$ , the constant  $\rho_0 = \rho(0)$  is selected such that  $\rho_0 > |e(0)|$ , the constant  $\rho_\infty = \lim_{t \rightarrow \infty} \rho(t)$  represents the maximum allowable size of the tracking error  $e(t)$  at the steady state and finally the decreasing rate of  $\rho(t)$ , which is affected by the constant  $l$  in this case, introduces a lower bound on the required speed of convergence of  $e(t)$ .

#### D. Dynamical Systems

Consider the initial value problem:

$$\dot{\xi} = h(t, \xi), \quad \xi(0) = \xi^0 \in \Omega_\xi \quad (10)$$

with  $h: \mathcal{R}_+ \times \Omega_\xi \rightarrow \mathcal{R}^n$  where  $\Omega_\xi \subset \mathcal{R}^n$  is a non-empty open set.

**Definition 1:** [16] A solution  $\xi(t)$  of the initial value problem (10) is maximal if it has no proper right extension that is also a solution of (10).

**Theorem 1:** [16] Consider the initial value problem (10). Assume that  $h(t, \xi)$  is: a) locally Lipschitz on  $\xi$  for almost all  $t \in \mathcal{R}_+$ , b) piecewise continuous on  $t$  for each fixed  $\xi \in \Omega_\xi$  and c) locally integrable on  $t$  for each fixed  $\xi \in \Omega_\xi$ . Then, there exists a maximal solution  $\xi(t)$  of (10) on the time interval  $[0, \tau_{\max})$  with  $\tau_{\max} > 0$  such that  $\xi(t) \in \Omega_\xi, \forall t \in [0, \tau_{\max})$ .

**Proposition 1:** [16] Assume that the hypotheses of Theorem 1 hold. For a maximal solution  $\xi(t)$  on the time interval  $[0, \tau_{\max})$  with  $\tau_{\max} < \infty$  and for any compact set  $\Omega'_\xi \subset \Omega_\xi$  there exists a time instant  $t' \in [0, \tau_{\max})$  such that  $\xi(t') \notin \Omega'_\xi$ .

### III. METHODOLOGY

Let  $x_d(t), y_d(t), z_d(t)$  and  $\psi_d(t)$  denote a desired smooth and bounded trajectory as well as yaw orientation respectively. The objective of this paper is to design a controller, without incorporating any information regarding the vehicle model, such that: a) it tracks the desired trajectory with the desired orientation via bounded closed loop signals and b) it achieves prescribed transient and steady state performance, despite the presence of exogenous disturbances representing ocean currents and waves.

#### A. Control Scheme

Let us define the position errors:

$$e_x = x - x_d, \quad e_y = y - y_d, \quad e_z = z - z_d \quad (11)$$

as well as the orientation error:

$$e_\psi = \psi - \psi_d. \quad (12)$$

Given the desired trajectory  $x_d(t), y_d(t), z_d(t)$  and orientation  $\psi_d(t)$  as well as the position/orientation errors (11)-(12):

#### I. Kinematic Controller

Select the exponentially decaying position/orientation performance functions  $\rho_x(t), \rho_y(t), \rho_z(t), \rho_\psi(t)$  that i) satisfy:

a. $ e_x(0)  < \rho_x(0)$	$0 < \rho_x(t)$	$0 < \lim_{t \rightarrow \infty} \rho_x(t)$
b. $ e_y(0)  < \rho_y(0)$	$0 < \rho_y(t)$	$0 < \lim_{t \rightarrow \infty} \rho_y(t)$
c. $ e_z(0)  < \rho_z(0)$	$0 < \rho_z(t)$	$0 < \lim_{t \rightarrow \infty} \rho_z(t)$
d. $ e_\psi(0)  < \rho_\psi(0)$	$0 < \rho_\psi(t)$	$0 < \lim_{t \rightarrow \infty} \rho_\psi(t)$

and ii) incorporate the desired performance specifications regarding the steady state error and the speed of convergence; and design the desired velocities:

$$\begin{bmatrix} u_d \\ v_d \\ w_d \end{bmatrix} = \begin{bmatrix} \cos \psi & -\sin \psi & 0 \\ \sin \psi & \cos \psi & 0 \\ 0 & 0 & 1 \end{bmatrix}^{-1} \begin{bmatrix} -k_x \frac{e_x}{\rho_x(t)} \\ -k_y \frac{e_y}{\rho_y(t)} \\ -k_z \frac{e_z}{\rho_z(t)} \end{bmatrix} \quad (13)$$

$$r_d = -k_\psi \frac{e_\psi}{\rho_\psi(t)} \quad (14)$$

with positive control gains  $k_x, k_y, k_z, k_\psi$ .

#### II. Dynamic Controller

Select exponentially decreasing velocity performance functions  $\rho_u(t), \rho_v(t), \rho_w(t), \rho_r(t)$  that satisfy:

a. $ u(0) - u_d(0)  < \rho_u(0)$	$0 < \rho_u(t)$	$0 < \lim_{t \rightarrow \infty} \rho_u(t)$
b. $ v(0) - v_d(0)  < \rho_v(0)$	$0 < \rho_v(t)$	$0 < \lim_{t \rightarrow \infty} \rho_v(t)$
c. $ w(0) - w_d(0)  < \rho_w(0)$	$0 < \rho_w(t)$	$0 < \lim_{t \rightarrow \infty} \rho_w(t)$
d. $ r(0) - r_d(0)  < \rho_r(0)$	$0 < \rho_r(t)$	$0 < \lim_{t \rightarrow \infty} \rho_r(t)$

and design the external forces in the surge, sway and heave as well as the external torque around yaw as:

$$X = -k_u \frac{u - u_d}{\rho_u(t)}, \quad Y = -k_v \frac{v - v_d}{\rho_v(t)}, \quad Z = -k_w \frac{w - w_d}{\rho_w(t)}, \quad N = -k_r \frac{r - r_d}{\rho_r(t)} \quad (15)$$

with positive control gains  $k_u, k_v, k_w, k_r$ .

**Remark 1:** The proposed control scheme does not incorporate the vehicle's dynamic model parameters or knowledge of the external disturbances. Furthermore, no estimation (i.e., adaptive control) has been employed to acquire such knowledge. Moreover, compared with the traditional backstepping-like approaches, the proposed methodology proves significantly less complex. Notice that no hard calculations are required to output the proposed control signals thus making its implementation straightforward.

#### B. Stability Analysis

The main results of this work are summarized in the following theorem where it is proven that the aforementioned control scheme solves the tracking control problem presented at the beginning of this section.

**Theorem 2:** Consider: i) the underwater vehicle model (1)-(8), ii) the desired trajectory  $x_d(t), y_d(t), z_d(t)$  and orientation  $\psi_d(t)$  and iii) the position/orientation errors defined in (11)-(12). The proposed control scheme (13)-(15) guarantees

that the vehicle tracks the desired trajectory and orientation with prescribed transient and steady state performance.

*Proof:* First, let us define the normalized errors:

$$\xi_x = \frac{e_x}{\rho_x(t)}, \xi_y = \frac{e_y}{\rho_y(t)}, \xi_z = \frac{e_z}{\rho_z(t)}, \xi_\psi = \frac{e_\psi}{\rho_\psi(t)} \quad (16)$$

$$\xi_u = \frac{u - u_d}{\rho_u(t)}, \xi_v = \frac{v - v_d}{\rho_v(t)}, \xi_w = \frac{w - w_d}{\rho_w(t)}, \xi_r = \frac{r - r_d}{\rho_r(t)} \quad (17)$$

and the overall closed loop system state vector as:

$$\xi = [\xi_x, \xi_y, \xi_z, \xi_\psi, \xi_u, \xi_v, \xi_w, \xi_r]^T.$$

Differentiating the normalized errors with respect to time and substituting (1)-(8) as well as (13)-(15), we obtain in a compact form, the dynamical system of the overall state vector:

$$\dot{\xi} = h(t, \xi) \quad (18)$$

where the function  $h(t, \xi)$  includes all terms found at the right hand side after the differentiation of  $\xi$ . Let us also define the open set:

$$\Omega_\xi = \underbrace{(-1, 1) \times \cdots \times (-1, 1)}_{8\text{-times}}.$$

The proof proceeds in two phases. First, the existence of a maximal solution  $\xi(t)$  of (18) over the set  $\Omega_\xi$  for a time interval  $[0, \tau_{\max})$  (i.e.,  $\xi(t) \in \Omega_\xi, \forall t \in [0, \tau_{\max})$ ) is ensured. Then, we prove that the proposed control scheme guarantees, for all  $t \in [0, \tau_{\max})$ : a) the boundedness of all closed loop signals as well as that b)  $\xi(t)$  remains strictly within a compact subset of  $\Omega_\xi$ , which subsequently will lead by contradiction to  $\tau_{\max} = \infty$ . Hence, from (16), we may conclude that:

$$\begin{aligned} -\rho_x(t) &< e_x(t) < \rho_x(t) \\ -\rho_y(t) &< e_y(t) < \rho_y(t) \\ -\rho_z(t) &< e_z(t) < \rho_z(t) \\ -\rho_\psi(t) &< e_\psi(t) < \rho_\psi(t) \end{aligned}$$

for all  $t \geq 0$  and consequently that tracking with prescribed performance is achieved as stated at the beginning of the section.

**Phase A.** The set  $\Omega_\xi$  is nonempty and open. Moreover, owing to the selection of the performance functions  $\rho_i(t)$  (i.e.,  $|e_i(0)| < \rho_i(0)$ ),  $i \in \{x, y, z, \psi, u, v, w, r\}$  we conclude that  $\xi(0) \in \Omega_\xi$ . Additionally, due to the smoothness of a) the system nonlinearities and b) the proposed control scheme, over  $\Omega_\xi$ , it can be easily verified that  $h(t, \xi)$  is continuous on  $t$  and continuous for all  $\xi \in \Omega_\xi$ . Therefore, the hypotheses of Theorem 1 stated in Subsection II-D hold and the existence of a maximal solution  $\xi(t)$  of (18) on a time interval  $[0, \tau_{\max})$  such that  $\xi(t) \in \Omega_\xi, \forall t \in [0, \tau_{\max})$  is ensured.

**Phase B.** We have proven in Phase A that  $\xi(t) \in \Omega_\xi, \forall t \in [0, \tau_{\max})$  or equivalently that:

$$\xi_i(t) \in (-1, 1), i \in \{x, y, z, \psi, u, v, w, r\} \quad (19)$$

for all  $t \in [0, \tau_{\max})$ . Therefore, the signals:

$$\varepsilon_i(t) = \ln \left( \frac{1 + \xi_i(t)}{1 - \xi_i(t)} \right), i \in \{x, y, z, \psi, u, v, w, r\} \quad (20)$$

are well defined for all  $t \in [0, \tau_{\max})$ . Consider now the positive definite and radially unbounded function  $V_p = \frac{1}{2}(\varepsilon_x^2 + \varepsilon_y^2 + \varepsilon_z^2)$ . Differentiating with respect to time and

substituting (1)-(3), we obtain:

$$\dot{V}_p = \left[ \frac{\varepsilon_x}{(1-\xi_x^2)\rho_x(t)}, \frac{\varepsilon_y}{(1-\xi_y^2)\rho_y(t)}, \frac{\varepsilon_z}{(1-\xi_z^2)\rho_z(t)} \right] \times \left( \begin{bmatrix} \cos \psi & -\sin \psi & 0 \\ \sin \psi & \cos \psi & 0 \\ 0 & 0 & 1 \end{bmatrix} \begin{bmatrix} u \\ v \\ w \end{bmatrix} + \begin{bmatrix} \delta_x(t) - \dot{x}_d(t) - \xi_x \dot{\rho}_x(t) \\ \delta_y(t) - \dot{y}_d(t) - \xi_y \dot{\rho}_y(t) \\ \delta_z(t) - \dot{z}_d(t) - \xi_z \dot{\rho}_z(t) \end{bmatrix} \right).$$

Incorporating  $u = u_d + \xi_u \rho_u(t)$ ,  $v = v_d + \xi_v \rho_v(t)$ ,  $w = w_d + \xi_w \rho_w(t)$  from (17) and substituting  $u_d, v_d, w_d$  from (13),  $\dot{V}_p$  becomes:

$$\dot{V}_p = \left[ \frac{\varepsilon_x}{(1-\xi_x^2)\rho_x(t)}, \frac{\varepsilon_y}{(1-\xi_y^2)\rho_y(t)}, \frac{\varepsilon_z}{(1-\xi_z^2)\rho_z(t)} \right] \times \left( \begin{bmatrix} -k_x \xi_x + \delta_x(t) - \dot{x}_d(t) - \xi_x \dot{\rho}_x(t) + \cos(\psi) \xi_u \rho_u(t) - \sin(\psi) \xi_v \rho_v(t) \\ -k_y \xi_y + \delta_y(t) - \dot{y}_d(t) - \xi_y \dot{\rho}_y(t) + \sin(\psi) \xi_u \rho_u(t) + \cos(\psi) \xi_v \rho_v(t) \\ -k_z \xi_z + \delta_z(t) - \dot{z}_d(t) - \xi_z \dot{\rho}_z(t) + \xi_w \rho_w(t) \end{bmatrix} \right).$$

Furthermore, utilizing (19) and the fact that  $\dot{\rho}_x(t), \dot{\rho}_y(t), \dot{\rho}_z(t), \rho_u(t), \rho_v(t), \rho_w(t), \delta_x(t), \delta_y(t), \delta_z(t), \dot{x}_d(t), \dot{y}_d(t), \dot{z}_d(t)$  are bounded by construction and by assumption, we arrive at:

$$\begin{aligned} |\delta_x(t) - \dot{x}_d(t) - \xi_x \dot{\rho}_x(t) + \cos(\psi) \xi_u \rho_u(t) - \sin(\psi) \xi_v \rho_v(t)| &\leq \bar{F}_x \\ |\delta_y(t) - \dot{y}_d(t) - \xi_y \dot{\rho}_y(t) + \sin(\psi) \xi_u \rho_u(t) + \cos(\psi) \xi_v \rho_v(t)| &\leq \bar{F}_y \\ |\delta_z(t) - \dot{z}_d(t) - \xi_z \dot{\rho}_z(t) + \xi_w \rho_w(t)| &\leq \bar{F}_z \end{aligned}$$

for some positive constants  $\bar{F}_x, \bar{F}_y, \bar{F}_z$ . Moreover,  $\frac{1}{(1-\xi_x^2)}, \frac{1}{(1-\xi_y^2)}, \frac{1}{(1-\xi_z^2)} > 1$  and  $\rho_x(t), \rho_y(t), \rho_z(t) > 0$ . Therefore, employing the fact that  $\varepsilon_i$  and  $\xi_i$  have the same sign (see (20)),  $i \in \{x, y, z, \psi, u, v, w, r\}$ , we conclude that  $\dot{V}_p$  is negative when the following inequalities hold:  $|\xi_x(t)| > \frac{\bar{F}_x}{k_x}, |\xi_y(t)| > \frac{\bar{F}_y}{k_y}, |\xi_z(t)| > \frac{\bar{F}_z}{k_z}$ . Thus, if we select  $k_x, k_y, k_z$  such that  $\frac{\bar{F}_x}{k_x}, \frac{\bar{F}_y}{k_y}, \frac{\bar{F}_z}{k_z} < 1$  then it can be easily concluded that:

$$-1 < -\frac{\bar{F}_i}{k_i} \leq \xi_i(t) \leq \frac{\bar{F}_i}{k_i} < 1, i \in \{x, y, z\} \quad (21)$$

for all  $t \in [0, \tau_{\max})$ . Subsequently, following similar analysis with  $V_o = \frac{1}{2}\varepsilon_\psi^2$ , we arrive at:

$$-1 < -\frac{\bar{F}_\psi}{k_\psi} \leq \xi_\psi(t) \leq \frac{\bar{F}_\psi}{k_\psi} < 1 \quad (22)$$

for a positive constant  $\bar{F}_\psi$  and a gain  $k_\psi$  satisfying  $k_\psi > \bar{F}_\psi$ . Additionally, the desired velocities  $u_d, v_d, w_d, r_d$  remain bounded for all  $t \in [0, \tau_{\max})$ . Thus, invoking (17), the boundedness of  $u(t), v(t), w(t), r(t)$  for all  $t \in [0, \tau_{\max})$  is also deduced. Finally, differentiating (13) and (14) with respect to time and after some algebraic manipulations it is straightforward to obtain the boundedness of  $\dot{u}_d(t), \dot{v}_d(t), \dot{w}_d(t), \dot{r}_d(t), \forall t \in [0, \tau_{\max})$ .

Applying the aforementioned line of proof for the dynamic part of the vehicle (5)-(8), considering  $V_d = \frac{1}{2}(\varepsilon_u^2 + \varepsilon_v^2 + \varepsilon_w^2 + \varepsilon_r^2)$  and the proposed control law (15), we arrive at:

$$-1 < -\frac{\bar{F}_i}{k_i} \leq \xi_i(t) \leq \frac{\bar{F}_i}{k_i} < 1 \quad (23)$$

for some positive constants  $\bar{F}_i$  and control gains  $k_i$  satisfying  $k_i > \bar{F}_i, i \in \{u, v, w, r\}$  as well as at the boundedness of the control law (15) for all  $t \in [0, \tau_{\max})$ .

Up to this point, what remains to be shown is that  $\tau_{\max} = \infty$ . Notice that (21), (22) and (23) imply that  $\xi(t) \in \Omega'_\xi, \forall t \in [0, \tau_{\max})$ , where:

$$\Omega'_\xi = \prod_{i \in \{x, y, z, \psi, u, v, w, r\}} \left[ -\frac{\bar{F}_i}{k_i}, \frac{\bar{F}_i}{k_i} \right]$$

is a nonempty and compact set. Moreover, it can be easily verified that  $\Omega'_\xi \subset \Omega_\xi$  for  $k_i > \bar{F}_i$ ,  $i \in \{x, y, z, \psi, u, v, w, r\}$ . Hence, assuming  $\tau_{\max} < \infty$  and since  $\Omega'_\xi \subset \Omega_\xi$ , Proposition 1 in Subsection II-D dictates the existence of a time instant  $t' \in [0, \tau_{\max})$  such that  $\xi(t') \notin \Omega'_\xi$ , which is a clear contradiction. Therefore,  $\tau_{\max} = \infty$ . As a result, all closed loop signals remain bounded and moreover  $\xi(t) \in \Omega'_\xi \subset \Omega_\xi$ ,  $\forall t \geq 0$ . Additionally, from (16), (21) and (22), we conclude that:

$$-\rho_i(t) < -\frac{\bar{F}_i}{k_i}\rho_i(t) \leq e_i(t) \leq \frac{\bar{F}_i}{k_i}\rho_i(t) < \rho_i(t)$$

for  $i \in \{x, y, z, \psi\}$ ,  $\forall t \geq 0$  and consequently that prescribed performance is achieved, as presented in Subsection II-C. Finally, since the exponential decaying orientation performance function  $\rho_\psi(t)$  was designed such that  $\rho_\psi(0) < \psi_c$  then it follows that  $|e_\psi(t)| < \rho_\psi(t) < \psi_c$  for all  $t \geq 0$  (that is, the target lies in the camera's field of view for all  $t \geq 0$ ), which completes the proof.

*Remark 2:* From the aforementioned proof, it is worth noticing that the proposed control scheme achieves its goals without residing to the need of rendering  $\frac{\bar{F}_i}{k_i}$ ,  $i \in \{x, y, z, \psi, u, v, w, r\}$  arbitrarily small, through extreme values of the control gains  $k_i$ ,  $i \in \{x, y, z, \psi, u, v, w, r\}$ . In this respect, the actual tracking performance, which is determined by the performance functions  $\rho_x(t)$ ,  $\rho_y(t)$ ,  $\rho_z(t)$ ,  $\rho_\psi(t)$ , becomes isolated against model uncertainties thus extending the robustness of the proposed control scheme.

*Remark 3:* In this work, neglecting the pitch and roll degrees of freedom, we considered a simplified underwater vehicle model for the clarity of the presentation and owing to page limitations. However, due to the passivity of pitch and roll degrees of freedom, it can be easily deduced following a standard Input to State Stability (ISS) framework, that a complete model with all 6 DOFs can be handled, without altering the proposed control scheme. Actually, the aforementioned statement will be verified by the following experimental results with the Girona500 AUV.

#### IV. EXPERIMENTS

To illustrate the performance of the proposed control scheme, two experimental procedures were carried out: a) navigation and stabilization to a specific configuration, b) meandrus-like trajectory tracking. The experiments took place inside a water tank using the Girona500 AUV. A panel consisting of valves and handles located inside the pool was used as the visual target during the experiments and the navigation module described in subsection II-B was responsible for providing the state feedback to the closed loop system in both experiments. In order to create strong external disturbances to the system, a water jet mechanism was installed on the AUV 4 DoFs robotic manipulator. The water jet was installed on the second rotational DoF of the manipulator which was moving constantly in both experiments in order to create time-varying and multidirectional external disturbances, as shown in Fig. 3 and Fig. 5.

##### A. Navigation and Stabilization towards a specific configuration (control panel)

In this experiment, the vehicle starts from an arbitrary initial configuration in order to navigate and stabilize towards a specific configuration (in front of a control panel). During the motion, the vehicle is constantly under the effect of time-varying and multidirectional external disturbances caused by the water jet mechanism. The required transient and steady state specifications, (that is, maximum steady state position errors 0.05m, maximum steady state orientation error  $5^\circ$  and exponential convergence  $e^{-0.1t}$ ), are described by the following performance functions:  $\rho_x(t) = (4.5 - 0.05)e^{-0.1t} + 0.05$ ,  $\rho_y(t) = (3.0 - 0.05)e^{-0.1t} + 0.05$ ,  $\rho_z(t) = (1 - 0.05)e^{-0.1t} + 0.05$ ,  $\rho_\psi(t) = (85 - 5)e^{-0.1t} + 5$ ,  $\rho_u(t) = (1 - 0.1)e^{-0.1t} + 0.1$ ,  $\rho_v(t) = (1 - 0.1)e^{-0.1t} + 0.1$ ,  $\rho_w(t) = (1 - 0.1)e^{-0.1t} + 0.1$ ,  $\rho_r(t) = (1 - 0.1)e^{-0.1t} + 0.1$ . Finally, the control gains were chosen as follows:  $k_x = 1$ ,  $k_y = 0.5$ ,  $k_z = 0.5$ ,  $k_\psi = 0.5$ ,  $k_u = 15$ ,  $k_v = 7.5$ ,  $k_w = 15$ ,  $k_r = 7.5$ .

The tracking error evolution is depicted in Fig. 2. The red lines indicate the desired performance bounds and the blue lines indicate the evolution of the tracking errors  $e_x(t)$ ,  $e_y(t)$ ,  $e_z(t)$  and  $e_\psi(t)$  respectively. All the errors have met the transient and steady state specifications imposed by the previously selected performance functions. As it can be seen from the results, the control objective has been achieved under the influence of external disturbances.

##### B. Meandrus-like Trajectory Tracking

In this experiment, the vehicle starts from an arbitrary initial configuration in order to perform a meandrus-like trajectory tracking under the effect of time-varying and multidirectional external disturbances. The required transient and steady state specifications are the same with the previous experiment. Therefore, we employed the same performance functions and control gains in the control scheme.

The tracking error evolution during the steady state is depicted in Fig. 4. The red lines indicate the desired performance bounds and the blue lines indicate the evolution of the tracking errors  $e_x(t)$ ,  $e_y(t)$ ,  $e_z(t)$  and  $e_\psi(t)$  respectively. As it is demonstrated by the experiments and predicted from the theoretical analysis, the control objective has been achieved in the presence of external disturbances.

#### V. CONCLUSIONS

This paper describes the design and implementation of a novel trajectory tracking control scheme for an Autonomous Underwater Vehicle (AUV). The proposed control scheme does not utilize the vehicle's dynamic model parameters and guarantees prescribed transient and steady state performance despite the presence of external disturbances. The proposed scheme is of low complexity and has analytically guaranteed stability and convergence properties, while its applicability and performance were experimentally verified using the Girona500 AUV operating under time-varying external disturbances towards two missions: a) navigation

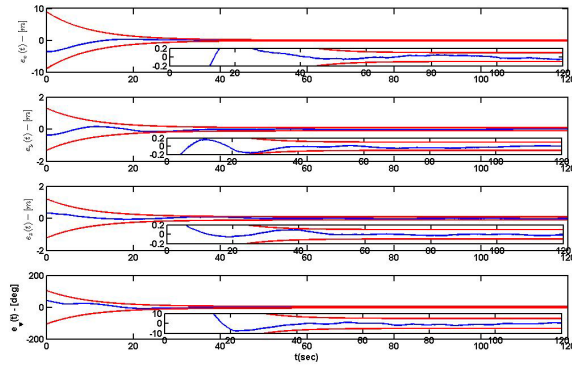


Fig. 2. Tracking error evolution during navigation and stabilization towards a specific configuration. The red lines indicate the desired performance bounds. The blue lines indicate the evolution of  $e_x(t)$ ,  $e_y(t)$ ,  $e_z(t)$  and  $e_\psi(t)$

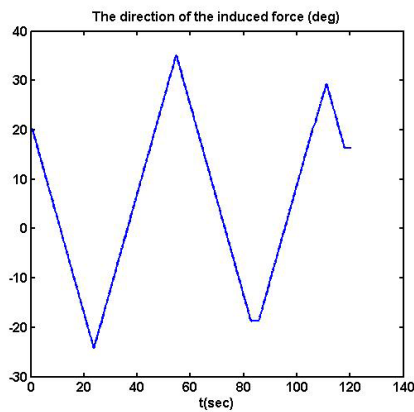


Fig. 3. Direction of the external disturbance induced by the water jet during the navigation and stabilization towards a specific configuration.

and stabilization to a specific configuration and b) trajectory tracking of a meandrus-like trajectory.

## REFERENCES

- [1] T. I. Fossen, *Guidance and Control of Ocean Vehicles*. Chichester, U.K.: Wiley, 1994.
- [2] T. J. Koo and S. Sastry, "Output tracking control design of a helicopter model based on approximate linearization," *Proceedings of the IEEE Conference on Decision and Control*, vol. 4, pp. 3635–3640, 1998.
- [3] S. A. Al-Hiddabi and N. H. McClamroch, "Tracking and maneuver regulation control for nonlinear nonminimum phase systems: Application to flight control," *IEEE Transactions on Control Systems Technology*, vol. 10, no. 6, pp. 780–792, 2002.
- [4] J. R. T. Lawton, R. W. Beard, and B. J. Young, "A decentralized approach to formation maneuvers," *IEEE Transactions on Robotics and Automation*, vol. 19, no. 6, pp. 933–941, 2003.
- [5] F. Alonge, F. D'Ippolito, and F. M. Raimondi, "Trajectory tracking of underactuated underwater vehicles," in *Proceedings of the IEEE Conference on Decision and Control*, vol. 5, 2001, pp. 4421–4426.
- [6] A. P. Aguiar and J. P. Hespanha, "Position tracking of underactuated vehicles," in *Proceedings of the American Control Conference*, vol. 3, 2003, pp. 1988–1993.
- [7] A. Baviskar, M. Feemster, D. Dawson, and B. Xian, "Tracking control of an underactuated unmanned underwater vehicle," in *Proceedings of the American Control Conference*, vol. 6, 2005, pp. 4321–4326.
- [8] F. Repoulas and E. Papadopoulos, "Planar trajectory planning and tracking control design for underactuated auvs," *Ocean Engineering*, vol. 34, no. 11–12, pp. 1650–1667, 2007.
- [9] A. P. Aguiar and J. P. Hespanha, "Trajectory-tracking and path-following of underactuated autonomous vehicles with parametric modeling uncertainty," *IEEE Transactions on Automatic Control*, vol. 52, no. 8, pp. 1362–1379, 2007.
- [10] A. P. Aguiar and A. M. Pascoal, "Dynamic positioning and way-point tracking of underactuated auvs in the presence of ocean currents," *International Journal of Control*, vol. 80, no. 7, pp. 1092–1108, 2007.
- [11] M. Santhakumar and T. Asokan, "Investigations on the hybrid tracking control of an underactuated autonomous underwater robot," *Advanced Robotics*, vol. 24, no. 11, pp. 1529–1556, 2010.
- [12] T. I. Fossen, *Guidance and Control of Ocean Vehicles*. Wiley, New York, 1994.
- [13] C. P. Bechlioulis and G. A. Rovithakis, "Robust adaptive control of feedback linearizable mimo nonlinear systems with prescribed performance," *IEEE Transactions on Automatic Control*, vol. 53, no. 9, pp. 2090–2099, 2008.
- [14] —, "Adaptive control with guaranteed transient and steady state tracking error bounds for strict feedback systems," *Automatica*, vol. 45, no. 2, pp. 532–538, 2009.
- [15] —, "Prescribed performance adaptive control for multi-input multi-output affine in the control nonlinear systems," *IEEE Transactions on Automatic Control*, vol. 55, no. 5, pp. 1220–1226, 2010.
- [16] E. D. Sontag, *Mathematical Control Theory*. London, U.K.: Springer, 1998.

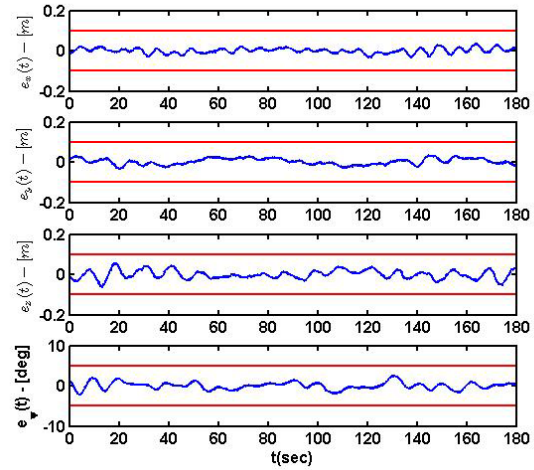


Fig. 4. Tracking error evolution during meandrus-like trajectory. The red lines indicate the desired performance bounds. The blue lines indicate the evolution of  $e_x(t)$ ,  $e_y(t)$ ,  $e_z(t)$  and  $e_\psi(t)$

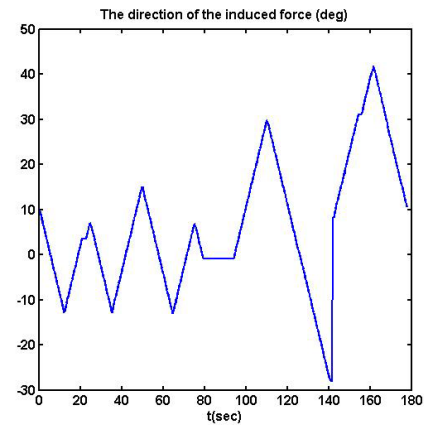


Fig. 5. Direction of the external disturbance induced by the water jet during the meandrus-like trajectory tracking.